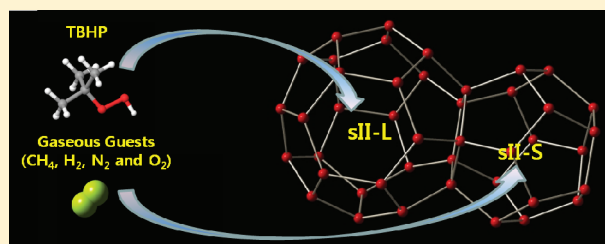


Phase Equilibria and Spectroscopic Identification of (2-Methylpropane-2-peroxol + Gaseous Guests) Hydrates

Minjun Cha, Minchul Kwon, Yeobum Youn, Kyuchul Shin,[†] and Huen Lee^{*}

Department of Chemical and Biomolecular Engineering (BK21 Program) and Graduate School of EEWS, Korea Advanced Institute of Science and Technology (KAIST), 335 Gwahangno, Yuseong-gu, Daejeon 305-701, Republic of Korea

ABSTRACT: In this study, we introduce a new structure-II hydrate former, 2-methylpropane-2-peroxol (*tert*-butyl hydroperoxide, TBHP), and identify the structure and guest distributions through spectroscopic tools including high-resolution powder diffraction (HRPD), ¹³C solid-state NMR, and Raman spectroscopy. Here, the (H + L + V) phase equilibrium data of (TBHP + X) hydrates (X = CH₄, N₂, and O₂) were measured at (3.3 to 7.56) MPa and (282.2 to 288.5) K for CH₄, (4.0 to 8.5) MPa and (271.6 to 277.5) K for N₂, and (4.0 to 8.6) MPa and (273.8 to 279.6) K for O₂. The (TBHP + X) hydrate phase equilibria showed that the addition of TBHP increased the structural stability with lower hydrate dissociation pressures when compared with those of pure CH₄, N₂, and O₂ hydrates. However, we noticed that the TBHP did not promote hydrate formation conditions as effectively as tetrahydrofuran.



INTRODUCTION

Clathrate hydrates¹ have received much attention recently due to their possible applications in areas such as gas separation,² carbon dioxide capture and sequestration (CCS),^{3,4} and energy-related devices (hydrogen gas sensors and proton conductors).^{5,6} Moreover, recent structure II (sII) hydrate-related findings such as the vacant cage generation via hydrate structure transition in nitrogen-doped ionic hydrate,⁷ plastic-like thermal deformation patterns,⁸ magnetic properties induced by selective guest injection,⁹ and large alcohol guest molecules inclusion in the large cage of sII hydrate (a molecular size above 0.75 nm)¹⁰ can contribute to clathrate hydrates being considered as quite promising functional materials.

Recent research reported an interesting phenomenon for large alcohol guest molecules.^{10–12} It was reported that some alcohols, such as 3-methyl-1-butanol (0.904 nm) and 2,2-dimethyl-1-propanol (0.776 nm), acted as sII formers in the presence of CH₄ as a help gas.¹⁰ We particularly note that Raman spectroscopy indicates an absence of a free OH peak for binary (3-methyl-1-butanol + CH₄) and (2,2-dimethyl-1-propanol + CH₄) hydrates.¹⁰ This information is useful for a better understanding of the nature of the guest–host system. At this stage, it might be worthwhile to determine whether the enclathration of the large guest molecule, 2-methylpropane-2-peroxol (*tert*-butyl hydroperoxide, TBHP) containing the peroxy group (–O–O–), can form the sII hydrate or not in the presence of a help gas such as methane, nitrogen, oxygen, and hydrogen.

In this study, we synthesized and measured the hydrate phase equilibria of binary 2-methylpropane-2-peroxol (*tert*-butyl hydroperoxide, TBHP) + X hydrates (X = CH₄, N₂, and O₂). Their structures and guest distributions were identified through spectroscopic measurements of high-resolution powder diffraction (HRPD), ¹³C solid-state NMR, and Raman spectroscopy. Additionally, we checked for the possible occurrence of a tuning pattern^{13–15} in the (TBHP + H₂) hydrate.

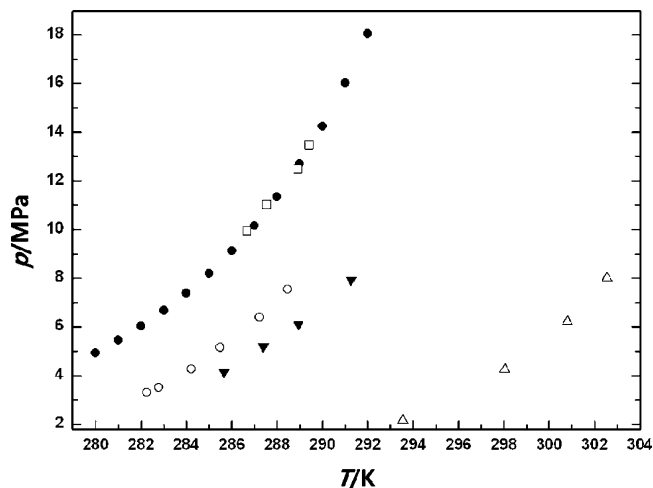


Figure 1. Pressure–temperature diagram for the 2-methylpropane-2-peroxol (*tert*-butyl hydroperoxide, TBHP, 0.0588 mole fraction of TBHP) + water + CH₄ system, the tetrahydrofuran (THF) + water + CH₄ system, the 2-methyl-2-propanol (*tert*-butyl alcohol, TBA) + water + CH₄ system, and pure CH₄ hydrates: ○, TBHP + CH₄ hydrate; ▼, TBA + CH₄ hydrate;²⁰ ●, pure CH₄ hydrate;¹⁹ □, pure CH₄ hydrate (in this study); △, THF + CH₄²¹ hydrate.

EXPERIMENTAL SECTION

Materials. CH₄, O₂, N₂, and H₂ gases were purchased from Special Gas (Korea) with stated minimum purities of 0.99995, 0.9995, 0.99999, and 0.9995 mole fractions, respectively. The 2-methylpropane-2-peroxol (*tert*-butyl hydroperoxide, TBHP,

Received: October 28, 2011

Accepted: February 28, 2012

Published: March 13, 2012

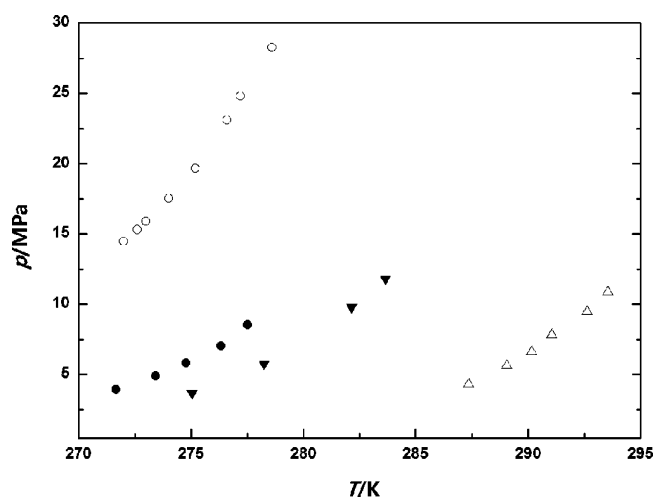


Figure 2. Pressure–temperature diagram for the 2-methylpropane-2-peroxol (*tert*-butyl hydroperoxide, TBHP, 0.0588 mole fraction of TBHP) + water + N₂ system, the tetrahydrofuran (THF) + water + N₂ system, the 1,4-dioxane + water + N₂ system, and pure N₂ hydrates: ○, pure N₂ hydrate;²² ▼, 1,4-dioxane + N₂ hydrate;²¹ ●, TBHP + N₂ hydrate; △, THF + N₂ hydrate.²¹

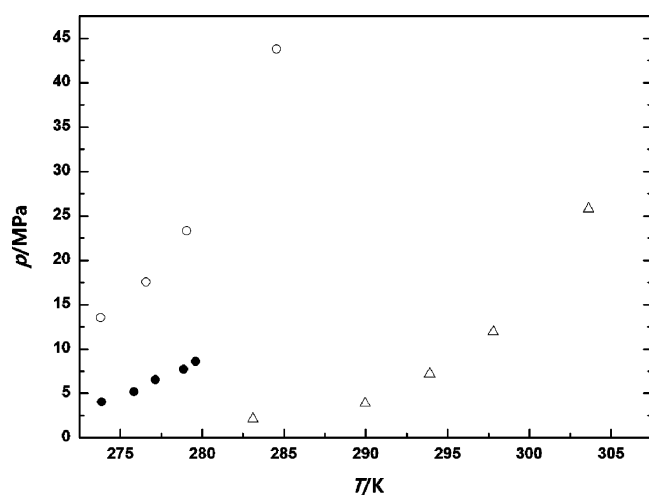


Figure 3. Pressure–temperature diagram for the 2-methylpropane-2-peroxol (*tert*-butyl hydroperoxide, TBHP, 0.0588 mole fraction of TBHP) + water + O₂ system, the tetrahydrofuran (THF) + water + O₂ system, and pure O₂ hydrates: ○, pure O₂ hydrate;²² ●, TBHP + O₂ hydrate; △, THF + O₂ hydrate.¹⁷

C₄H₁₀O₂, 0.7 weight fraction in water) was supplied by Tokyo Chemical Industry (TCI). All chemicals were used without any further purification. Ultrahigh purity water was obtained from a Millipore purification unit.

Methods. We adopted well-defined routine procedures¹⁶ to measure the hydrate phase equilibria of the CH₄, N₂, and O₂ + TBHP + H₂O samples. First, the TBHP solution (0.0588 mole fraction) was introduced into an equilibrium vessel (with an effective volume of 150 mL) equipped with a mechanical stirrer and a K-type thermocouple probe with a calibrated digital thermometer (Barnant 90) with an uncertainty of ± 0.05 K and then immersed into an alcohol bath (Jeio Tech., RW-2025G) with an uncertainty factor of ± 0.05 K. A digital pressure gauge (DPI 104, 0 to 14 MPa) with full-scale accuracy of 0.05 % was used to check the cell pressure continuously. After the TBHP solution was introduced into the high-pressure reactor, the

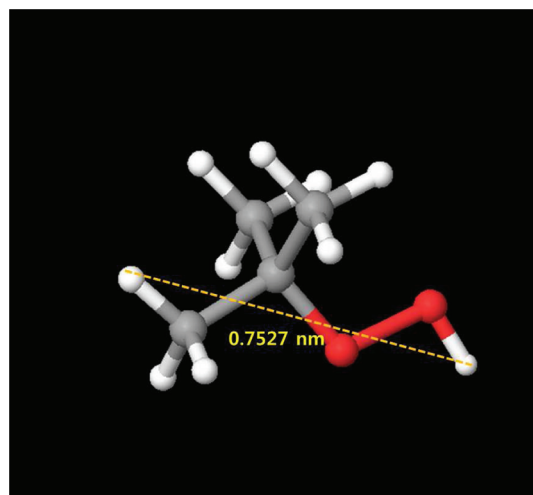


Figure 4. Calculated structure and end-to-end distance of 2-methylpropane-2-peroxol (*tert*-butyl hydroperoxide, TBHP).

Table 1. Phase (H + L + V) Equilibria of the Binary (TBHP + CH₄) Hydrate

T/K	p/MPa	T/K	p/MPa
282.25	3.30	282.77	3.51
284.21	4.27	285.49	5.16
287.23	6.40	288.47	7.56

Table 2. Phase (H + L + V) Equilibria of the Binary (TBHP + N₂) Hydrate

T/K	p/MPa	T/K	p/MPa
271.66	3.95	273.43	4.92
274.78	5.85	276.33	7.02
277.51	8.54		

Table 3. Phase (H + L + V) Equilibria of the Binary (TBHP + O₂) Hydrate

T/K	p/MPa	T/K	p/MPa
273.85	4.02	275.85	5.21
277.15	6.50	278.87	7.73
279.58	8.62		

pressure-vessel was pressurized to the desired level by supplying gas (CH₄, N₂, and O₂). When the system temperature and pressure were stable, the system temperature was gradually decreased to 263.15 K (at a rate of 1.0 K·h⁻¹), and hydrate formation was indicated by a sudden pressure drop. After hydrate formation, the cell temperature was slowly elevated at a rate of 0.1 K·h⁻¹ to dissociate the formed hydrate. The pressure–temperature trace during hydrate formation and dissociation was measured to determine the dissociation points of the (TBHP + X) hydrates (X = CH₄, N₂, and O₂). The point at which the slope of the pressure–temperature curve changed sharply is considered to be the dissociation points at which all hydrate structures disappeared.^{17,18}

For the present experiments, a liquid solution of TBHP (0.0588 mole fraction) was made by adding ultra high-purity water to a TBHP solution (0.7 weight fraction in water, Sigma-Aldrich, Inc.), freezing the mixture at 213.15 K for at least one day, and finally grinding it to a fine powder (~200 μm).

This fine powder sample was placed into a precooled high pressure cell with a volume of 20 mL and was exposed to CH_4 , N_2 , and O_2 gas up to 12.0 MPa at 213 K for at least one week. For the binary (TBHP + hydrogen) hydrate samples, the precooled high-pressure cell containing a finely powdered solid mixture of ice and the promoter solution (solid ice + promoter mixture, 0.0588 mole fraction of TBHP, and 0.008 mole fraction of TBHP) was exposed to H_2 gas up to 70.0 MPa at 255 K. During the HRPD (Pohang Accelerator Laboratory, Beamline 8C2) measurements, a θ - $2\theta^{-1}$ scan mode with a fixed step size of 0.01° for $2\theta = (0 \text{ to } 120)^\circ$ and a fixed scan time of 2 s (with a wavelength of 0.15490 nm) were used for each sample at 80 K. Raman experiments (Horiba Jobin Yvon, France)

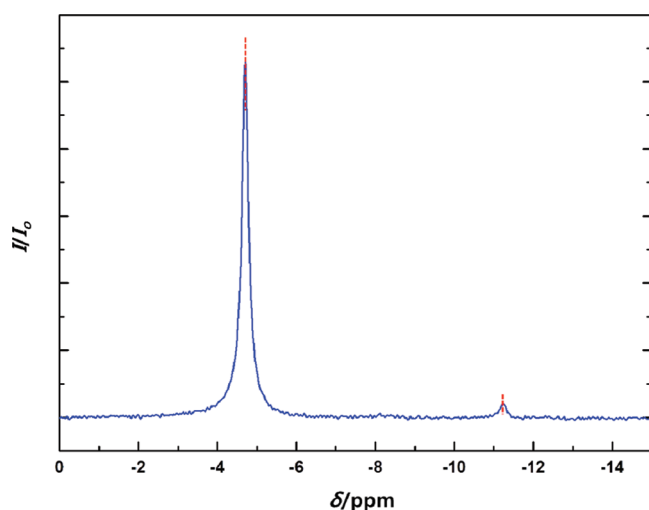


Figure 5. HPDEC ^{13}C NMR result of (0.0588 mole fraction of TBHP + water + CH_4 system) at 203.15 K, and TBHP hydrate sample was synthesized at 12.0 MPa and 213.15 K; peak at $\delta_{\text{C}} = -4.7$ ppm corresponding to CH_4 in sII-S (the small S^{12} cage in sII hydrate); peak at $\delta_{\text{C}} = -11.0$ ppm corresponding to CH_4 in vapor phase; I , relative NMR intensity; δ , chemical shift.

were performed using a CCD detector cooled by liquid nitrogen and an Ar-ion laser at 514.53 nm as the excitation source. The intensity of the laser was about 20 mW. The THMS600G model (Linkam stage) was used to cool the samples to 93.15 K in the Raman analysis. The solid-state NMR spectra of binary (TBHP + CH_4) hydrate samples at 203.15 K were recorded at a Larmor frequency of 100.6 MHz with MAS at approximately 5 kHz (Bruker AVANCE 400 MHz). A pulse length of $2 \mu\text{s}$ and a pulse repetition delay of 10 s under proton decoupling were employed with a radio frequency field strength of 50 kHz, corresponding to $5 \mu\text{s}$ 90° pulses. As an external chemical shift reference, the downfield carbon resonance peak of adamantane, assigned a chemical shift of 38.3 ppm at 298 K, was used.

RESULTS AND DISCUSSION

Hydrate Phase Equilibria for sII of (TBHP + X) Hydrates (X = CH_4 , N_2 , and O_2). The TBHP solution (0.0588 mole fraction, slightly in excess of the stoichiometric concentration, for all large cages to be filled, of the sII hydrate) was introduced into a high-pressure reactor, and the (H + L + V) phase equilibrium data of the (TBHP + X) hydrates (X = CH_4 , N_2 , and O_2) were measured at pressures ranging from (3.3 to 7.56) MPa and at temperatures ranging from (282.2 to 288.5) K for CH_4 , at pressures ranging from (4.0 to 8.5) MPa and at temperatures ranging from (271.6 to 277.5) K for N_2 , and at pressures ranging from (4.0 to 8.6) MPa and at temperatures ranging from (273.8 to 279.6) K for O_2 . As shown in Figure 1, the hydrate equilibrium pressures for the CH_4 + water + TBHP system are reduced dramatically compared to the those for pure CH_4 hydrate.¹⁹ However, the hydrate dissociation conditions in the CH_4 + water + TBHP system are higher than those in the CH_4 + water + tetrahydrofuran (THF, powerful sII hydrate former) system and the CH_4 + water + 2-methyl-2-propanol (*tert*-butyl alcohol, TBA, sII hydrate former with CH_4) system.^{20,21} Similar promoter effects and trends were observed for TBHP with N_2 and O_2 help guests (Figures 2 and 3).^{17,21,22} The thermodynamic stability of (TBHP + X) hydrates (X = N_2 and O_2) is

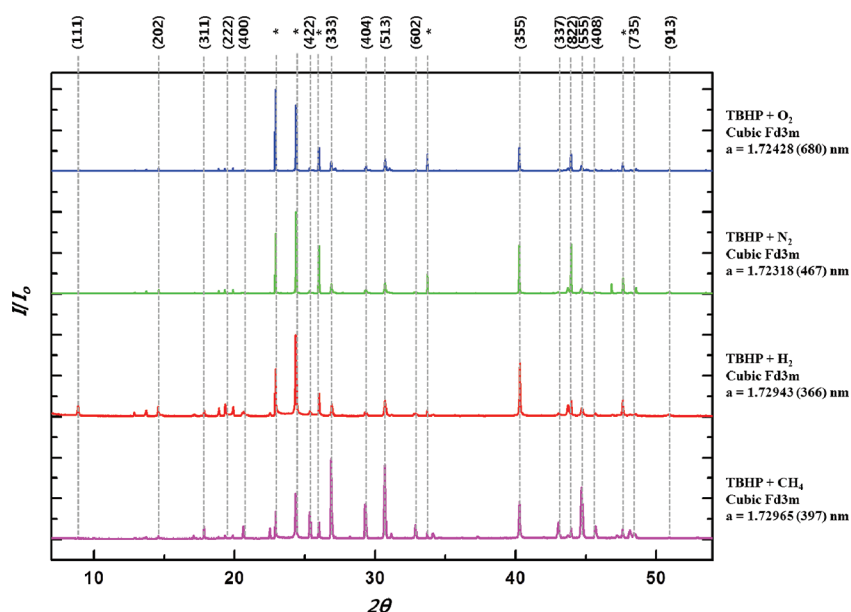


Figure 6. HRPD patterns of binary (TBHP + X) hydrates (X = CH_4 , N_2 , O_2 , and H_2) at 80 K. The diffraction peaks of hexagonal ice are marked by asterisks (*). Here the TBHP (0.0588 mole fraction) hydrate sample was synthesized at 12.0 MPa and 213.15 K; I , relative XRD intensity (magenta, CH_4 ; red, H_2 ; green, N_2 ; blue, O_2).

higher than those of pure CH_4 , N_2 , and O_2 hydrates. The resulting equilibrium data are plotted in Figures 1, 2, and 3 and are listed in Tables 1, 2, and 3.

Spectroscopic Identification of (TBHP + X) Hydrates ($X = \text{CH}_4$, N_2 , O_2 , and H_2). First, the optimum molecular structure of the TBHP molecule was determined by Maestro with the Jaguar application.^{23,24} The molecular size of the TBHP molecule needed to be determined first because it becomes one of the key factors for determining the hydrate structure. We used the B3LYP method with the 6-31++ basis set; this result is shown in Figure 4. The calculated molecular size of the TBHP molecule (0.7527 nm) implies that a structure H (sH) hydrate can be exclusively formed with a help gas.¹

The solid-state ^{13}C HPDEC NMR spectrum of the (TBHP + CH_4 + H_2O) hydrate sample is shown in Figure 5 at 203.15 K. However, we could identify only the peak at $\delta_{\text{C}} = -4.7$ ppm corresponding to CH_4 in sII-S (the small 5^{12} cage in sII hydrate).²⁵ This type of unusual inclusion of a peroxide guest molecule in sII hydrate appears to be quite similar to our previous results of large alcohol guest molecules (3-methyl-1-butanol and 2,2-dimethyl-1-propanol).¹⁰ The signal of the CH_4 peak at $\delta_{\text{C}} = -11.0$ ppm can be assigned to methane in the gas phase. Here, we could not observe a CH_4 peak at $\delta_{\text{C}} = -8.3$ ppm (large $5^{12}6^4$ cage, sII-L), implying that nearly all of the sII-L cages are occupied by large TBHP guest molecules.²⁵ The basic structure of the (TBHP + CH_4) hydrate sample was also identified by using the HRPD at 80 K as shown in Figure 6.

Recent studies have reported the gaseous guest-dependent (xenon and methane) hydrate structure for amyl alcohol hydrates (3-methyl-1-butanol).^{11,12} Ripmeester et al. confirmed that 3-methyl-1-butanol (molecular size: 0.906 nm) in the presence of xenon (Xe) forms the sH hydrate, while 3-methyl-1-butanol can form a sII hydrate with CH_4 as a help gas.^{11,12} Here, we also checked (TBHP + X) hydrate samples ($X = \text{N}_2$, O_2 , and H_2) through HRPD measurements to identify the possible occurrence of the gaseous guest-dependent hydrate structure induced by N_2 , O_2 , and H_2 gas. The HRPD patterns of the (TBHP + X) hydrate samples ($X = \text{N}_2$, O_2 , and H_2) were analyzed using the Chekcell program (Laugier)²⁶ and are shown in Figure 6. The structures of the (TBHP + X) hydrates ($X = \text{N}_2$, O_2 , and H_2) were identified to be cubic (space group of $Fd\bar{3}m$) with the lattice parameter of $a = 1.7296 (\pm 0.0039)$ nm for CH_4 , $a = 1.7294 (\pm 0.0036)$ nm for H_2 , $a = 1.7232 (\pm 0.0046)$ nm for N_2 , and $a = 1.7242 (\pm 0.0068)$ nm for O_2 hydrates at 80 K, respectively.²⁷ All of the calculated values have similar values of $a = 1.72$ nm, which are similar to sII THF hydrate at 140 K. The Miller indices of the (TBHP + X) hydrates ($X = \text{CH}_4$, N_2 , O_2 , and H_2) are also represented in Figure 6.²⁸ However, we did not observe the gaseous-guest dependent hydrate structure in binary (TBHP + X) hydrates ($X = \text{CH}_4$, N_2 , O_2 , and H_2). The unique inclusion of the relatively large peroxide guest (TBHP) into the sII hydrate framework has been confirmed here by solid-state NMR and HRPD.

As shown in Figures 7, 8, and 9, we identified using Raman spectroscopy (at 93.15 K) the unique gaseous-guest inclusion of binary (TBHP + X) hydrates ($X = \text{CH}_4$, N_2 , O_2 , and H_2) and observed no evidence of a free OH signal being in the (TBHP + X) hydrates ($X = \text{CH}_4$, N_2 , O_2 , and H_2). As clearly shown in Figure 7a, we obtained the representative peak of CH_4 molecules in small cages of sII hydrate at around 2914 cm^{-1} for the C–H stretching vibrational mode of CH_4 and the broad vibrational band of the O–H mode from the host-water frameworks at around 3150 cm^{-1} .¹ We also checked for the

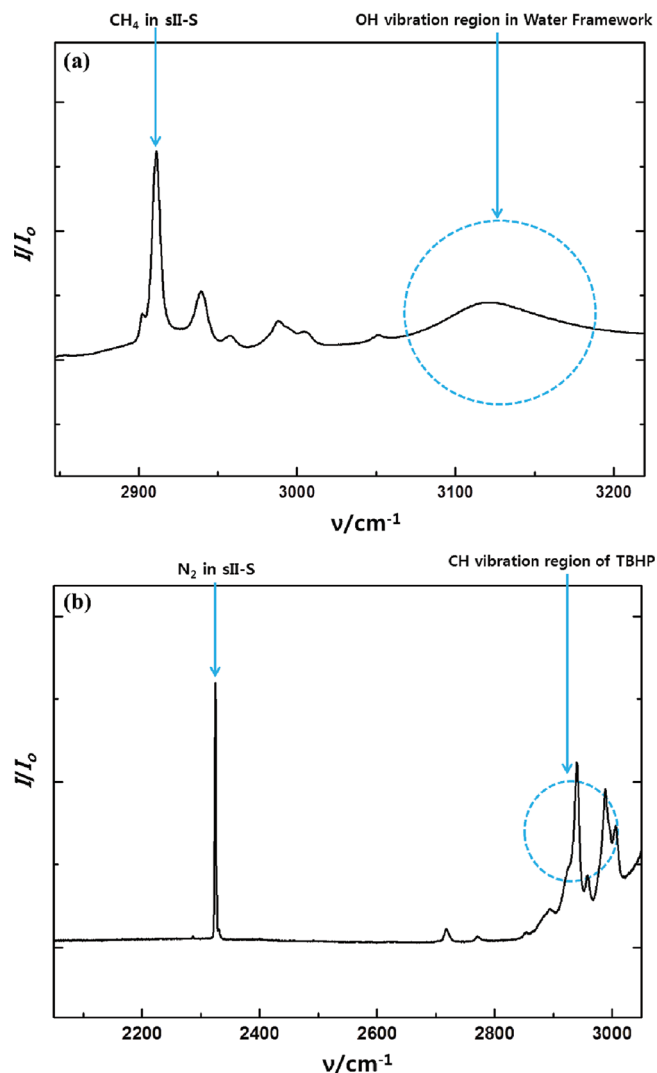


Figure 7. Raman spectra of binary (TBHP + X) hydrates ($X = \text{CH}_4$, N_2 , O_2 , and H_2) at 93.15 K in the range of (a) (2800 to 3200) cm^{-1} of (0.0588 mole fraction of TBHP + water + CH_4) hydrate, (b) (2050 to 3050) cm^{-1} of (0.0588 mole fraction of TBHP + water + N_2) hydrate. Here TBHP (0.0588 mole fraction) hydrate samples ($X = \text{CH}_4$, N_2 , and O_2) were synthesized at 12.0 MPa and 213.15 K, and the TBHP (0.0588 mole fraction and 0.008 mole fraction) + hydrogen hydrate sample was synthesized at 70.0 MPa and 255 K; I , relative Raman intensity; ν , Raman shift.

representative peaks of gaseous guest (N_2 , O_2 , and H_2) through Raman spectroscopy and identified these at around 2322 cm^{-1} for the N–N mode of N_2 (Figure 7b), 1546 cm^{-1} for the O–O mode of O_2 (Figure 8a), and (4119 and 4125) cm^{-1} (two peaks from the ortho–para transition hydrogen molecules in the hydrate cage, Figure 8b) for the H–H mode of H_2 in the small cages of the sII hydrate.¹ However, we failed to observe the non-hydrogen bonded O–H stretching signals, called the free OH bond, of TBHP at around 3600 cm^{-1} (Figure 9a).¹⁰ Normally, the ordinarily encaged large guest molecules (LGMs) containing the OH group in their hydrate cages have no hydrogen interaction with host–water frameworks and show the free OH signal in the Raman spectra.¹⁰ This fact strongly implies that the OH of TBHP closely interacts with the host–water frameworks.¹⁰ This type of OH interaction with the host frameworks appears to be quite similar to our previous results of 3-methyl-1-butanol and 2,2-dimethyl-1-propanol hydrates with CH_4 .¹⁰

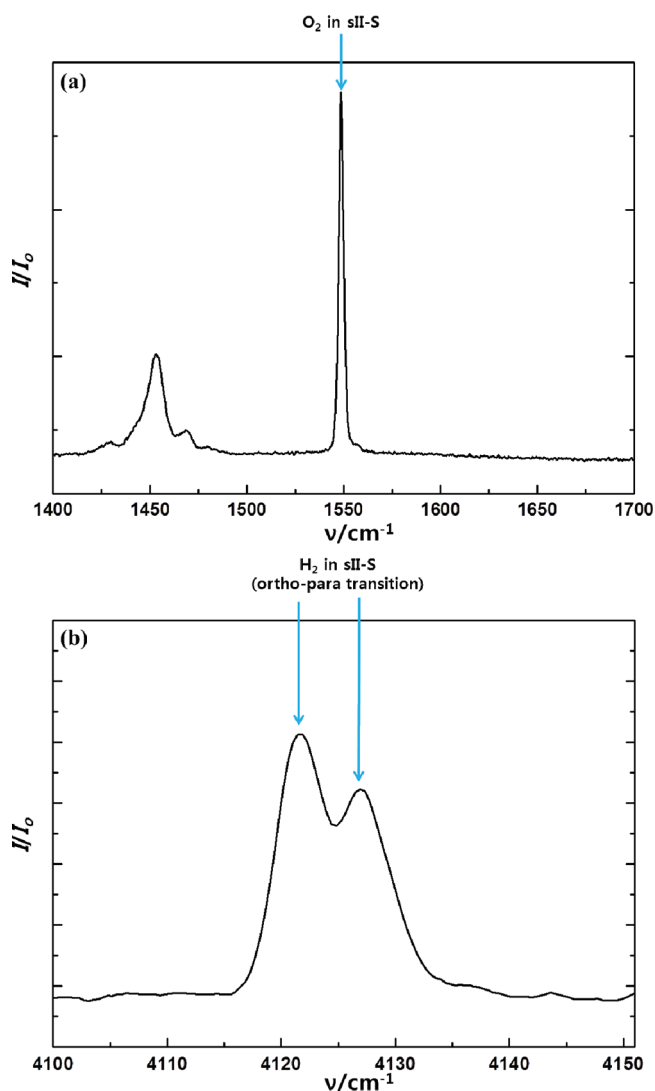


Figure 8. Raman spectra of binary (TBHP + X) hydrates ($X = \text{CH}_4$, N_2 , O_2 , and H_2) at 93.15 K in the range of (a) (1400 to 1800) cm^{-1} of (0.0588 mole fraction of TBHP + water + O_2) hydrate, (b) (4100 to 4150) cm^{-1} of (0.0588 mole fraction of TBHP + water + H_2) hydrate. Here TBHP (0.0588 mole fraction) hydrate samples ($X = \text{CH}_4$, N_2 , and O_2) were synthesized at 12.0 MPa and 213.15 K, and the TBHP (0.0588 mole fraction and 0.008 mole fraction) + hydrogen hydrate sample was synthesized at 70.0 MPa and 255 K; I , relative Raman intensity; ν , Raman shift.

Additionally, we checked for the possible occurrence of hydrogen tuning^{13–15} behavior in the binary (TBHP + H_2) hydrate. For the binary (TBHP + hydrogen) hydrate samples, the precooled high pressure cell containing a finely powdered solid mixture of ice and the promoter solution (solid ice + promoter mixture) is exposed to H_2 gas up to 70.0 MPa at 255 K (0.0588 mole fraction in the Raman spectra shown in Figure 8b and 0.008 mole fraction of the TBHP in the Raman spectra shown in Figure 9b). Lokshin et al.²⁹ reported that, under these pressure and temperature conditions, the pure hydrogen hydrate did not form; therefore, we were convinced that the large cage occupancies of hydrogen molecules in the binary TBHP (0.008 mole fraction of TBHP) + hydrogen hydrate were from tuning phenomenon (Figure 9b). We also conclude the absence of the H–H vibron in the large cages (occupied by 0.0588 mole fraction of TBHP, slightly in excess of the

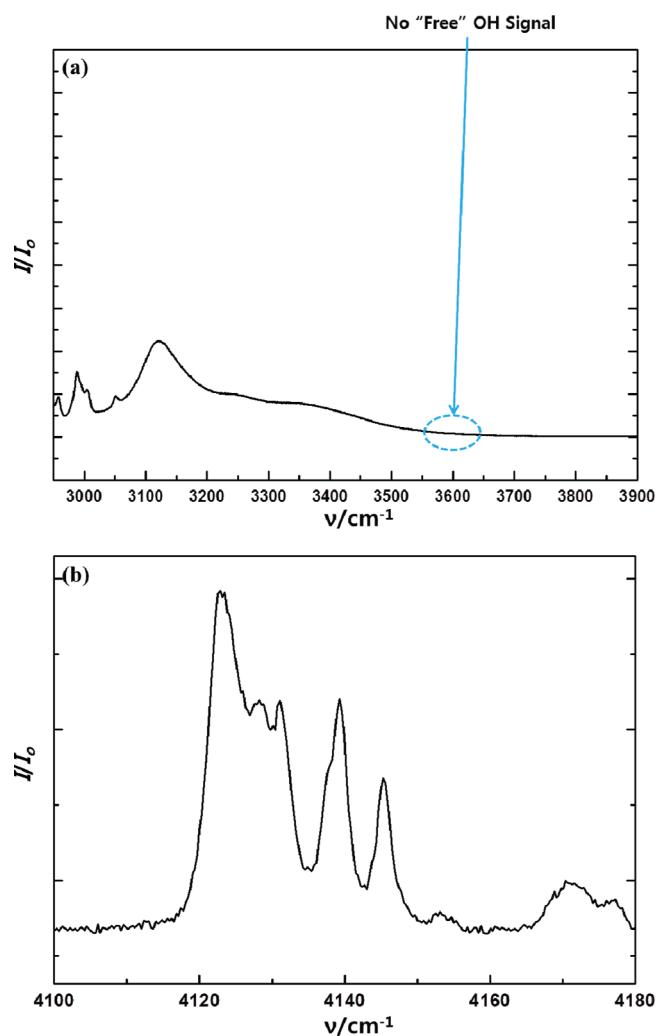


Figure 9. Raman spectra of binary (TBHP + X) hydrates ($X = \text{CH}_4$, N_2 , O_2 , and H_2) at 93.15 K in the range of (a) (2950 to 3900) cm^{-1} of (0.0588 mole fraction of TBHP + water + CH_4) hydrate, (b) (4100 to 4180) cm^{-1} of (0.008 mole fraction of TBHP + water + H_2) hydrate. Here TBHP (0.0588 mole fraction) hydrate samples ($X = \text{CH}_4$, N_2 , and O_2) were synthesized at 12.0 MPa and 213.15 K, and the TBHP (0.0588 mole fraction and 0.008 mole fraction) + hydrogen hydrate sample was synthesized at 70.0 MPa and 255 K; I , relative Raman intensity; ν , Raman shift.

stoichiometric concentration for all large cages to be filled) of sII hydrate in Figure 8b reveals no hydrogen tuning behavior occurring in (TBHP + H_2 hydrate).^{14,15,29} As shown in Figure 9b, we observed the H–H vibron peaks of large cages in the sII (TBHP + H_2) hydrate, which might give us a clear indication of the clusters of two, three, and four hydrogen molecules per large cage in the (0.008 mole fraction of TBHP + hydrogen hydrate).

CONCLUSIONS

In this study, we identified the structure and guest distributions of a new structure-II hydrate former, *tert*-butyl hydroperoxide, using the spectroscopic tools of high-resolution powder diffraction (HRPD) and ^{13}C solid-state NMR. The existence of free OH was checked by Raman spectroscopy and was found to be absent for these binary hydrates. We also checked for the possible occurrence of binary (TBHP + hydrogen) hydrate. Finally, we measured the hydrate phase equilibria of the binary (TBHP + X)

hydrates ($X = \text{CH}_4$, N_2 , and O_2) and compared their thermodynamic stability with the corresponding pure ones.

AUTHOR INFORMATION

Corresponding Author

*Tel.: +82-42-350-3917; fax: +82-42-350-3910; e-mail: h_lee@kaist.ac.kr.

Present Address

†National Research Council of Canada, 100 Sussex Drive, Ottawa K1A 0R6, Canada.

Funding

This research was supported by the National Research Foundation (NRF) of Korea grant (WCU program: 31-2008-000-10055-0 and Korea Government: 2010-0029176) funded by the Ministry of Education, Science and Technology (MEST). This research was also supported by the Ministry of Knowledge Economy through (Recovery/Production of Natural Gas Hydrate using Swapping Technique, KIGAM - Gas Hydrate R&D Organization). HRPD Experiments at PLS (Beamline 8C2) were supported in part by MEST and POSTECH.

Notes

The authors declare no competing financial interest.

REFERENCES

- (1) Sloan, E. D.; Koh, C. A. *Clathrate Hydrates of Natural Gases*, 3rd ed.; CRC Press: Boca Raton, FL, 2008.
- (2) Kang, S.-P.; Lee, H. Recovery of CO_2 from flue gas using gas hydrate: Thermodynamic verification through phase equilibrium measurements. *Environ. Sci. Technol.* **2000**, *34*, 4397–4400.
- (3) Lee, H.; Seo, Y.; Seo, T.-T.; Moudrakovski, I. L.; Ripmeester, J. A. Recovering Methane from Solid Methane Hydrate with Carbon Dioxide. *Angew. Chem., Int. Ed.* **2003**, *42* (41), 5048–5051.
- (4) Park, Y.; Kim, D.-Y.; Lee, J.-W.; Huh, D.-G.; Park, K.-P.; Lee, J.; Lee, H. Sequestering carbon dioxide into complex structures of naturally occurring gas hydrates. *Proc. Natl. Acad. Sci. U.S.A.* **2006**, *103* (34), 12690–12694.
- (5) Cha, J.-H.; Lee, W.; Lee, H. Thermal stability and ionic conductivity of the ionic clathrate hydrates incorporated with potassium hydroxide. *J. Mater. Chem.* **2009**, *19*, 6542–6547.
- (6) Cha, J.-H.; Lee, W.; Lee, H. Hydrogen Gas Sensor Based on Proton-Conducting Clathrate Hydrate. *Angew. Chem., Int. Ed.* **2009**, *121* (46), 8843–8846.
- (7) Shin, K.; Choi, S.; Cha, J.-H.; Lee, H. Structural Transformation due to Co-Host Inclusion in Ionic Clathrate Hydrates. *J. Am. Chem. Soc.* **2008**, *130* (23), 7180–7181.
- (8) Park, Y.; Choi, Y. N.; Yeon, S.-H.; Lee, H. Thermal Expansivity of Tetrahydrofuran Clathrate Hydrate with Diatomic Guest Molecules. *J. Phys. Chem. B* **2008**, *112*, 6897–6899.
- (9) Park, Y.; Dho, J.; Seol, J.; Yeon, S.-H.; Cha, M.; Jeong, Y. H.; Seo, Y.; Lee, H. Magnetic Transition and Long-Time Relaxation Behavior Induced by Selective Injection of Guest Molecules into Clathrate Hydrates. *J. Am. Chem. Soc.* **2009**, *131*, 5736–5737.
- (10) Cha, M.; Shin, K.; Lee, H. Spectroscopic Identification of Amyl Alcohol Hydrates through Free OH Observation. *J. Phys. Chem. B* **2009**, *113*, 10562–10565.
- (11) Ripmeester, J. A.; Ratcliffe, C. I. Xenon-129 NMR Studies of Clathrate Hydrates: New Guests for Structure II and Structure H. *J. Phys. Chem.* **1990**, *94*, 8773–8776.
- (12) Ohmura, R.; Takeya, S.; Uchida, T.; Ikeda, I. Y.; Ebinuma, T.; Narita, H. Clathrate hydrate formation in the system methane + 3-methyl-1-butanol + water: Equilibrium data and crystallographic structures of hydrates. *Fluid Phase Equilib.* **2004**, *221*, 151–156.
- (13) Lee, H.; Lee, J.; Kim, D. Y.; Park, J.; Seo, Y.-T.; Zeng, H.; Moudrakovski, I. L.; Ratcliffe, C. I.; Ripmeester, J. A. Tuning Clathrate Hydrates For Hydrogen Storage. *Nature* **2005**, *434*, 743–746.
- (14) Sugahara, T.; Haag, J. C.; Prasad, P. S. R.; Warntje, A. A.; Sloan, E. D.; Sum, A. K.; Koh, C. A. Increasing Hydrogen Storage Capacity Using Tetrahydrofuran. *J. Am. Chem. Soc.* **2009**, *131* (41), 14616–14617.
- (15) Sugahara, T.; Haag, J. C.; Warntje, A. A.; Prasad, P. S. R.; Sloan, E. D.; Koh, C. A.; Sum, A. K. Large-Cage Occupancies of Hydrogen in Binary Clathrate Hydrates Dependent on Pressures and Guest Concentrations. *J. Phys. Chem. C* **2010**, *114* (35), 15218–15222.
- (16) Ohgaki, K.; Makihara, Y.; Takano, K. Formation of CO_2 Hydrate in Pure and Sea Waters. *J. Chem. Eng. Jpn.* **1993**, *26*, 558–564.
- (17) Yang, H.; Fan, S.; Lang, X.; Wang, Y. Phase Equilibria of Mixed Gas Hydrates of Oxygen + Tetrahydrofuran, Nitrogen + Tetrahydrofuran, and Air + Tetrahydrofuran. *J. Chem. Eng. Data* **2011**, *56*, 4152–4156.
- (18) Tumba, K.; Reddy, P.; Naidoo, P.; Ramjugernath, D. Phase Equilibria of Methane and Carbon Dioxide Clathrate Hydrates in the Presence of Aqueous Solutions of Tributylmethylphosphonium Methylsulfate Ionic Liquid. *J. Chem. Eng. Data* **2011**, *56*, 3620–3629.
- (19) Deaton, W. M.; Frost, E. M. Jr. Gas Hydrates and Their Relation to the Operation of Natural Gas Pipelines. *U.S. Bur. Mines Monogr.* **1946**, *8*, 101.
- (20) Park, Y.; Cha, M.; Shin, W.; Lee, H.; Ripmeester, J. A. Spectroscopic Observation of Critical Guest Concentration appearing in *tert*-Butyl Alcohol Clathrate Hydrate. *J. Phys. Chem. B* **2008**, *112*, 8443–8446.
- (21) Seo, Y.-T.; Kang, S.-P.; Lee, H. Experimental Determination and Thermodynamic Modeling of Methane and Nitrogen Hydrates in the Presence of THF, Propylene Oxide, 1,4-Dioxane and Acetone. *Fluid Phase Equilib.* **2001**, *189*, 99–110.
- (22) Van Cleeff, A.; Diepen, G. A. M. Gas hydrates of N_2 and O_2 , II. *Rec. Trav. Chim.* **1960**, *79*, 582.
- (23) *Maestro*, version 9.2; Schrödinger, LLC: New York, 2011.
- (24) *Jaguar*, version 7.8; Schrödinger, LLC: New York, 2011.
- (25) Choi, S.; Shin, K.; Lee, H. Structure Transition and Tuning Pattern in the Double (Tetramethylammonium Hydroxide + Gaseous Guests) Clathrates. *J. Phys. Chem. B* **2007**, *111*, 10224–10230.
- (26) Laugier, J.; Bochu, B. Laboratoire des Matériaux et du Génie Physique, Ecole Supérieure de Physique de Grenoble. <http://www.ccp14.ac.uk> (accessed June 24, 2011).
- (27) Shin, K.; Cha, M.; Choi, S.; Dho, J.; Lee, H. Discrete Magnetic Patterns of Nonionic and Ionic Clathrate Hydrates. *J. Am. Chem. Soc.* **2008**, *130* (51), 17234–17235.
- (28) Jones, C. Y.; Marchall, S. L.; Chakoumakos, B. C.; Rawn, C. J.; Ishii, Y. Structure and Thermal Expansivity of Tetrahydrofuran Deuterate Determined by Neutron Powder Diffraction. *J. Phys. Chem. B* **2003**, *107*, 6026–6031.
- (29) Lokshin, K. A.; Zhao, Y.; He, D.; Mao, W. L.; Mao, H.-K.; Hemley, R.; Lobanov, M. V.; Greenblatt, M. Structure and Dynamics of Hydrogen Molecules in the Novel Clathrate Hydrate by High Pressure Neutron Diffraction. *Phys. Rev. Lett.* **2004**, *125*503.